Taylor-Hood B-spline elements for the Isogeometric Analysis of the Navier-Stokes equations

Babak S. Hosseini[1], Matthias Möller[2], Stefan Turek[1]

[1]Institute of Applied Mathematics, LS III
TU Dortmund
babak.hosseini@math.tu-dortmund.de

[2]Delft Institute of Applied Mathematics
Delft University of Technology

TU Delft, 12.03.2015

Table of Contents

Overview

Motivation

- Industrial FEM simulation workflow: Model design with CAD[1] software $\rightarrow$ Model transformation $\rightarrow$ Analysis $\rightarrow$ Postprocessing
- Standard modeling technology in CAD: NURBS
- Increasingly more complex engineering designs (Submarine: $\geq 1.000.000$ parts)
- CAD-CAE[2] bottleneck: Efficient creation of 'simulation-specific' geometry
- Design to Analysis workflow: $80\%/20\%$ modeling/analysis time ratio

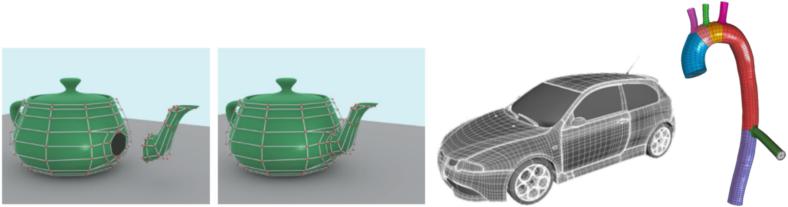

Figure : NURBS geometries taken from [1, 2, 3]

[1] Computer-aided design
[2] Computer-aided engineering

Motivation

- Demand for greater precision and tighter integration of modeling-analysis process
  - Automatic and adaptive mesh refinement requires access to the exact geometry
  - Design optimization
  - Uncertainty quantification
- FEM mesh only an approximation of the CAD geometry
  - Shell buckling analysis very sensitive to geometric imperfections
  - Boundary layer phenomena sensitive to precise geometry of aerodynamic and hydrodynamic configurations
  - Sliding contact between bodies cannot be accurately represented without precise geometric descriptions
- Limited number of $\mathcal{C}^{>0}$ FE applicable to complex geometries already in 2D

T.J.R. Hughes et al.:
'*Isogeometric Analysis was motivated by the existing gap between the worlds of finite element analysis (FEA) and computer-aided design (CAD)*' [4]

Overview

Galerkin based Isogeometric Analysis (IGA) in a nutshell

- CAD and Analysis use the same geometric model (NURBS, T-splines, etc.)
- Isoparametric concept: Use the same class of functions used in CAD (B-splines, NURBS, etc.) for the PDE solution space
- Generalization of standard FEA: NURBS spaces include the piecewise polynomial spaces used in FEA
- Possibility for $\mathcal{C}^1$ and higher order continuity
- Higher-order accuracy on the degree-of-freedom basis
- Compact support
- Two- and three-dimensional geometric flexibility

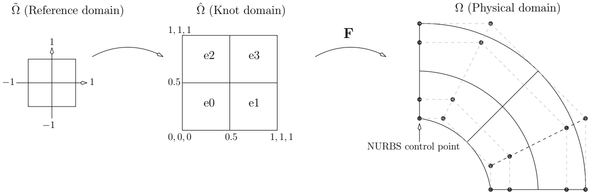

Figure : Domains involved in Isogeometric Analysis.

B-splines/NURBS in a nutshell

Define ordered knot vector $\Xi := \{\xi_1, \xi_2, \dots, \xi_{m=n+p+1}\}$, where p is the polynomial degree, n is the number of B-spline basis functions and repetitions of knots ξ_i are allowed: $\xi_1 \leq \xi_2 \leq \cdots \leq \xi_m$.

Ξ is an open knot vector, i.e., first and last knots have multiplicities $p+1$: $\Xi = \{\underbrace{a, \dots, a}_{p+1}, \xi_{p+2}, \dots, \xi_{m-p-1}, \underbrace{b, \dots, b}_{p+1}\}$.

i-th univariate B-spline function is a piecewise polynomial function, recursively defined by the Cox-de Boor recursion formula

$$B_{i,0}(\xi) = \begin{cases} 1, & \text{if } \xi_i \leq \xi < \xi_{i+1} \\ 0, & \text{otherwise} \end{cases}$$

$$B_{i,p}(\xi) = \frac{\xi - \xi_i}{\xi_{i+p} - \xi_i} B_{i,p-1}(\xi) + \frac{\xi_{i+p+1} - \xi}{\xi_{i+p+1} - \xi_{i+1}} B_{i+1,p-1}(\xi), \quad p > 0.$$

B-splines/NURBS in a nutshell

- B-spline basis functions are linearly independent and form a partition of unity: $\sum_{i=1}^{n} B_{i,p}(\xi) = 1 \ \ \forall \xi \in \Xi$
- Each B-spline basis function is non-negative over entire domain: $B_{i,p}(\xi) \geq 0, \forall \xi$
- Local support property: $B_{i,p}(\xi) = 0$, if ξ outside the interval $[\xi_i, \xi_{i+p+1})$
- On each segment, we have p+1 basis functions with positive values
- At knot ξ_i the basis functions have $\alpha := p - r_i$ continuous derivatives, where r_i denotes the multiplicity of knot ξ_i

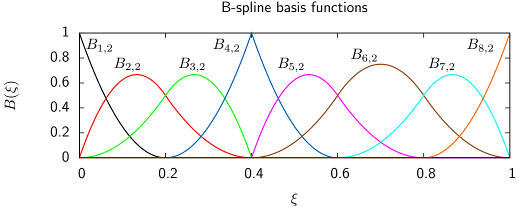

Figure : B-spline basis functions of degree $p = 2$ for open knot vector $\Xi := \{0, 0, 0, 0.2, 0.4, 0.4, 0.6, 0.8, 1, 1, 1\}$.

B-splines/NURBS in a nutshell

Derivative of i-th B-spline basis function obtained combining lower order ones:

$$\frac{d}{d\xi}B_{i,p}(\xi) = \frac{p}{\xi_{i+p} - \xi_i}B_{i,p-1}(\xi) - \frac{p}{\xi_{i+p+1} - \xi_{i+1}}B_{i+1,p-1}(\xi).$$

Augment B-splines $B_{i,p}$ with with weights w_i to obtain univariate **NURBS** basis functions (rational B-splines):

$$R_{i,p}(\xi) = \frac{B_{i,p}(\xi)w_i}{W(\xi)}, \qquad W(\xi) = \sum_{j=1}^{n} B_{j,p}(\xi)w_j.$$

First derivative of $R_{i,p}(\xi)$ is easily obtained via the quotient rule as:

$$\frac{d}{d\xi}R_{i,p}(\xi) = w_i \frac{B'_{i,p}(\xi)W(\xi) - B_{i,p}(\xi)W'(\xi)}{W^2(\xi)},$$

where $B'_{i,p}(\xi) = \frac{d}{d\xi}B_{i,p}(\xi)$ and $W'(\xi) = \sum_{i=1}^{n} B'_{i,p}(\xi)w_i$.

B-splines/NURBS in a nutshell

Space of B-splines/NURBS of degree p and regularity α determined by knot vector Ξ and spanned by the basis functions $B_{i,p}/R_{i,p}$:

$$\mathcal{S}^p_\alpha \equiv \mathcal{S}^p_\alpha(\Xi, p) := \operatorname{span}\{B_{i,p}\}_{i=1}^n$$
$$\mathcal{N}^p_\alpha \equiv \mathcal{N}^p_\alpha(\Xi, p, w) := \operatorname{span}\{R_{i,p}\}_{i=1}^n$$

Extension to higher dimensions

Consider d knot vectors Ξ_β, $1 \leq \beta \leq d$ and an open parametric domain $(a_d, b_d)^d \in \mathbb{R}^d$. The knot vectors Ξ_β partition the parametric domain $(a_d, b_d)^d$ into d-dimensional open knot spans, or elements, and thus yield a mesh $\mathcal{Q}$ being defined as

$$\mathcal{Q} \equiv \mathcal{Q}(\Xi_1, \ldots, \Xi_d) := \{Q = \otimes_{\beta=1}^d (\xi_{i,\beta}, \xi_{i+1,\beta}) \mid Q \neq \emptyset,\ 1 \leq i \leq m_\beta\}$$

Tensor product B-spline and NURBS basis functions:

$$B_{i_1,\ldots,i_d} := B_{i_1,1} \otimes \cdots \otimes B_{i_d,d}, \quad i_1 = 1, \ldots, n_1, \quad i_d = 1, \ldots, n_d$$

$$R_{i_1,\ldots,i_d} := R_{i_1,1} \otimes \cdots \otimes R_{i_d,d}, \quad i_1 = 1, \ldots, n_1, \quad i_d = 1, \ldots, n_d$$

B-splines/NURBS in a nutshell

$$B_{i,j}^{p,q}(\xi,\eta) = B_{i,p}(\xi)B_{j,q}(\eta)$$

$$\frac{\partial B_{i,j}^{p,q}(\xi,\eta)}{\partial \xi} = \frac{d}{d\xi}\Big(B_{i,p}(\xi)\Big)B_{j,q}(\eta), \quad \frac{\partial B_{i,j}^{p,q}(\xi,\eta)}{\partial \eta} = B_{i,p}(\xi)\frac{d}{d\eta}\Big(B_{j,q}(\eta)\Big)$$

$$R_{i,j}^{p,q}(\xi,\eta) = \frac{B_{i,p}(\xi)B_{j,q}(\eta)w_{i,j}}{\sum_{i=1}^{n}\sum_{j=1}^{m} B_{i,p}(\xi)B_{j,q}(\eta)w_{i,j}}$$

$$\frac{\partial R_{i,j}^{p,q}(\xi,\eta)}{\partial \xi} = w_{i,j}\frac{B'_{i,p}(\xi)B_{j,q}(\eta)W(\xi,\eta) - B_{i,p}(\xi)B_{j,q}(\eta)W'_{\xi}(\xi,\eta)}{W^2(\xi,\eta)}$$

$$\frac{\partial R_{i,j}^{p,q}(\xi,\eta)}{\partial \eta} = w_{i,j}\frac{B_{i,p}(\xi)B'_{j,q}(\eta)W(\xi,\eta) - B_{i,p}(\xi)B_{j,q}(\eta)W'_{\eta}(\xi,\eta)}{W^2(\xi,\eta)}$$

$$W'_{\xi}(\xi,\eta) = \sum_{i=1}^{n}\sum_{j=1}^{m} B'_{i,p}(\xi)B_{j,q}(\eta)w_{i,j}, \quad W'_{\eta}(\xi,\eta) = \sum_{i=1}^{n}\sum_{j=1}^{m} B_{i,p}(\xi)B'_{j,q}(\eta)w_{i,j}$$

$$W(\xi,\eta) = \sum_{i=1}^{n}\sum_{j=1}^{m} B_{i,p}(\xi)B_{j,q}(\eta)w_{i,j}$$

B-splines/NURBS in a nutshell

Tensor product B-spline and NURBS spaces

$$\mathcal{S}^{p_1,\dots,p_d}_{\alpha_1,\dots,\alpha_d} \equiv \mathcal{S}^{p_1,\dots,p_d}_{\alpha_1,\dots,\alpha_d}(\mathcal{Q}) := \mathcal{S}^{p_1}_{\alpha_1} \otimes \dots \otimes \mathcal{S}^{p_d}_{\alpha_d} = \operatorname{span}\{B_{i_1\dots i_d}\}_{i_1=1,\dots,i_d=1}^{n_1,\dots,n_d}$$

$$\mathcal{N}^{p_1,\dots,p_d}_{\alpha_1,\dots,\alpha_d} \equiv \mathcal{N}^{p_1,\dots,p_d}_{\alpha_1,\dots,\alpha_d}(\mathcal{Q}) := \mathcal{N}^{p_1}_{\alpha_1} \otimes \dots \otimes \mathcal{N}^{p_d}_{\alpha_d} = \operatorname{span}\{R_{i_1\dots i_d}\}_{i_1=1,\dots,i_d=1}^{n_1,\dots,n_d}$$

Spaces fully characterized by mesh $\mathcal{Q}$, degrees $p_1,\dots,p_d$ of basis functions and their continuities $\alpha_1,\dots,\alpha_d$.

Representation in the physical domain Ω

NURBS geometrical map $\mathbf{F} : \hat{\Omega} \to \Omega$

$$\mathbf{F} = \sum_{i_1=1}^{n_1} \cdots \sum_{i_d=1}^{n_d} R_{i_1}(\xi_{i_1}) \dots R_{i_d}(\xi_{i_d}) \mathbf{P}_{i_1,\dots,i_d}$$

Space $\mathcal{V}$ of NURBS basis functions on Ω, as *push-forward* of space $\mathcal{N}$

$$\mathcal{V}^{p_1,\dots,p_d}_{\alpha_1,\dots,\alpha_d} := \mathcal{V}^{p_1}_{\alpha_1} \otimes \dots \otimes \mathcal{V}^{p_d}_{\alpha_d} = \operatorname{span}\{R_{i_1\dots i_d} \circ \mathbf{F}^{-1}\}_{i_1=1,\dots,i_d=1}^{n_1,\dots,n_d}$$

B-splines/NURBS in a nutshell

[3]**,,bent" Sobolev space** of order $m \in \mathbb{N}$

$$\mathcal{H}^m := \begin{cases} v \in L^2(\hat{\Omega}) \text{ such that} \\ v_{|Q} \in H^m(Q), \forall Q \in \mathcal{Q}, \text{ and} \\ \nabla^k(v_{|Q_1}) = \nabla^k(v_{|Q_2}) \text{ on } \partial Q_1 \cap \partial Q_2, \\ \forall k \in \mathbb{N} \text{ with } 0 \leq k \leq \min\{m_{Q_1,Q_2}, m-1\} \\ \forall Q_1, Q_2 \text{ with } \partial Q_1 \cap \partial Q_2 \neq \emptyset \end{cases}$$

with norm

$$\|v\|^2_{\mathcal{H}^m} := \sum_{i=0}^{m} |v|^2_{\mathcal{H}^i}$$

and seminorms

$$|v|^2_{\mathcal{H}^i} := \sum_{Q \in \mathcal{Q}} |v|^2_{H^i(Q)}, \ 0 \leq i \leq m$$

[3]Continuity may vary throughout the domain

Approximation with NURBS in the physical domain

Fundamental error estimate for the elliptic boundary value problem in classical FEA:

$$\left\|u - u^h\right\|_m \leq C h^\beta \left\|u\right\|_r, \quad \beta = \min(p+1-m, r-m)$$

Mesh $\mathcal{K}$ in the physical space: $\mathcal{K} = \mathbf{F}(Q) := \{\mathbf{F}(\boldsymbol{\xi}) | \boldsymbol{\xi} \in Q\}$.

Theorem ([5])

Let k and l be integer indices with $0 \leq k \leq l \leq p+1$, we have

$$\sum_{K \in \mathcal{K}_h} |v - \Pi_{\mathcal{V}_h} v|^2_{H^k(K)} \leq C_{shape} \sum_{K \in \mathcal{K}_h} h_K^{2(l-k)} \sum_{i=0}^{l} \|\nabla \boldsymbol{F}\|^{2(i-l)}_{L^\infty(\boldsymbol{F}^{-1}(K))} |v|^2_{H^i(K)},$$

$\forall v \in H^l(\Omega)$

Remark [5]

The NURBS space $\mathcal{V}_h$ on the physical domain Ω delivers the optimal rate of convergence, as for the classical finite element spaces of degree p.

Approximation with NURBS in the physical domain

Example: Poisson problem on a quarter ring (with exact solution [6])

$$\text{find } u : \Omega \to \mathbb{R} : \begin{cases} -\nabla \cdot (\mu \nabla u) = f & \text{in } \Omega \\ u = g & \text{on } \Gamma_D \\ \mu \nabla u \cdot \boldsymbol{n} = h & \text{on } \Gamma_N \end{cases}$$

$$f(x,y) = \frac{4}{(x^2+y^2)^4}[12x^2y^2(x^2+y^2)^2 - 2(x^2+y^2)^4 + 2(r_{\mathsf{in}}+r_{\mathsf{out}})(x^2+y^2)^{7/2} - 15(r_{\mathsf{in}}+r_{\mathsf{out}})x^2y^2(x^2+y^2)^{3/2} - 2r_{\mathsf{in}}r_{\mathsf{out}}(x^6 - 5x^4y^2 - 5x^2y^4 + y^6)]$$

$$u(x,y) = \frac{4x^2y^2}{(x^2+y^2)^2}[x^2+y^2-(r_{\mathsf{in}}+r_{\mathsf{out}})(x^2+y^2)^{1/2} + r_{\mathsf{in}}r_{\mathsf{out}}]$$

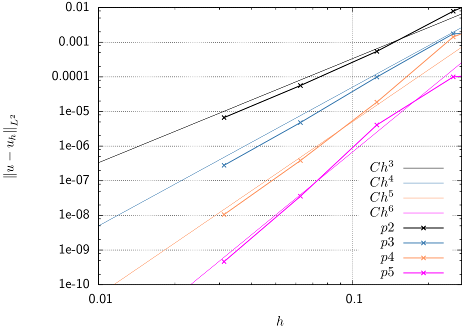

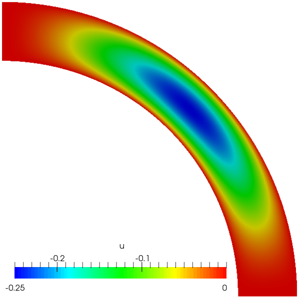

Smooth generalizations of Taylor-Hood like B-spline space pairs

Approximation of velocity and pressure functions with LBB-stable Taylor-Hood like B-spline space pairs $\hat{\mathbf{V}}_h^{TH}/\hat{Q}_h^{TH}$

$$\hat{\mathbf{V}}_h^{TH} \equiv \hat{\mathbf{V}}_h^{TH}(\mathbf{p},\boldsymbol{\alpha}) = \boldsymbol{\mathcal{S}}_{\alpha_1,\alpha_2}^{p_1+1,p_2+1} = \mathcal{S}_{\alpha_1,\alpha_2}^{p_1+1,p_2+1} \times \mathcal{S}_{\alpha_1,\alpha_2}^{p_1+1,p_2+1}$$
$$\hat{Q}_h^{TH} \equiv \hat{Q}_h^{TH}(\mathbf{p},\boldsymbol{\alpha}) = \mathcal{S}_{\alpha_1,\alpha_2}^{p_1,p_2}$$

Corresponding spaces $\mathbf{V}_h^{TH}$ and Q_h^{TH} in the physical domain Ω obtained via component wise mapping using parameterization $\mathbf{F}:\hat{\Omega}\to\Omega$

$$\mathbf{V}_h^{TH} = \{\mathbf{v} : \mathbf{v}\circ\mathbf{F} \in \hat{\mathbf{V}}_h^{TH}\} \qquad Q_h^{TH} = \{q : q\circ\mathbf{F} \in \hat{Q}_h^{TH}\}$$

Spaces may be set up to use NURBS instead of B-spline basis functions.

Overview

Governing equations

Steady-state incompressible Navier-Stokes equations in strong form:

$$
\begin{aligned}
-\nu\nabla^2\boldsymbol{v} + (\boldsymbol{v}\cdot\nabla)\boldsymbol{v} + \nabla p &= \boldsymbol{b} && \text{in } \Omega \\
\nabla\cdot\boldsymbol{v} &= 0 && \text{in } \Omega \\
\boldsymbol{v} &= \boldsymbol{v}_D && \text{on } \Gamma_D \\
-p\boldsymbol{n} + \nu(\boldsymbol{n}\cdot\nabla)\boldsymbol{v} &= \boldsymbol{t} && \text{on } \Gamma_N
\end{aligned}
$$

- $\Omega \subset \mathbb{R}^2$ is a bounded domain
- density $\rho = 1$
- kinematic viscosity $\nu = \mu/\rho$, dynamic viscosity μ
- normalized pressure $p = P/\rho$
- body force term $\boldsymbol{b}$
- $\boldsymbol{v}_D$: velocity Dirichlet boundary condition on Dirichlet boundary Γ_D
- $\boldsymbol{t}$: prescribed traction force on Neumann boundary Γ_N
- $\boldsymbol{n}$: outward unit normal vector on domain boundary

Governing equations

Continuous mixed variational formulation: Find $\boldsymbol{v} \in \boldsymbol{\mathcal{H}}^1_{\Gamma_D}(\Omega)$ and $p \in \mathcal{L}_2(\Omega)/\mathbb{R}$ such that for all $(\boldsymbol{w}, q) \in \boldsymbol{\mathcal{H}}^1_0(\Omega) \times \mathcal{L}_2(\Omega)/\mathbb{R}$ it holds

$$\begin{cases} a(\boldsymbol{w},\boldsymbol{v}) + c(\boldsymbol{v};\boldsymbol{w},\boldsymbol{v}) + b(\boldsymbol{w},p) = \ (\boldsymbol{w},\boldsymbol{b}) + (\boldsymbol{w},\boldsymbol{t})_{\Gamma_N} \\ b(\boldsymbol{v},q) = 0 \end{cases}$$

$$\underbrace{\nu \int_\Omega \nabla \boldsymbol{w} \ : \nabla \boldsymbol{v} \, \mathrm{d}\Omega}_{a(\boldsymbol{w},\boldsymbol{v})} + \underbrace{\int_\Omega \boldsymbol{w} \cdot \boldsymbol{v} \cdot \nabla \boldsymbol{v} \, \mathrm{d}\Omega}_{c(\boldsymbol{v};\boldsymbol{w},\boldsymbol{v})} - \underbrace{\int_\Omega \nabla \cdot \boldsymbol{w} \, p \, \mathrm{d}\Omega}_{b(\boldsymbol{w},p)} - \underbrace{\int_\Omega q \, \nabla \cdot \boldsymbol{v} \, \mathrm{d}\Omega}_{b(\boldsymbol{v},q)} =$$

$$\underbrace{\int_\Omega \boldsymbol{w} \cdot \boldsymbol{b} \, \mathrm{d}\Omega}_{(\boldsymbol{w},\boldsymbol{b})} + \underbrace{\int_{\partial\Omega} \nu \, \boldsymbol{w} \cdot (\nabla \boldsymbol{v} \cdot \boldsymbol{n}) \, \mathrm{d}\partial\Omega}_{(\boldsymbol{w},\boldsymbol{t})_{\Gamma_N}} - \int_{\partial\Omega} p \, \boldsymbol{w} \cdot \boldsymbol{n} \mathrm{d}\partial\Omega$$

Discrete problem:

$$\begin{cases} \text{Find } \ \boldsymbol{v}^h \in \boldsymbol{\mathcal{H}}^1_{\Gamma_D}(\Omega) \cap \mathbf{V}_h^{TH} \ \text{ and } \ p^h \in \mathcal{L}_2(\Omega)/\mathbb{R} \cap Q_h^{TH}, \text{such that} \\ \forall (\boldsymbol{w}^h, q^h) \in \boldsymbol{\mathcal{H}}^1_0(\Omega) \cap \mathbf{V}_h^{TH} \times \mathcal{L}_2(\Omega)/\mathbb{R} \cap Q_h^{TH} \\ a(\boldsymbol{w}^h,\boldsymbol{v}^h) + c(\boldsymbol{v}^h;\boldsymbol{w}^h,\boldsymbol{v}^h) + b(\boldsymbol{w}^h,p^h) = \ (\boldsymbol{w}^h,\boldsymbol{b}^h) + (\boldsymbol{w}^h,\boldsymbol{t}^h)_{\Gamma_N} \\ b(\boldsymbol{v}^h,q^h) = 0 \end{cases}$$

Governing equations

Treatment of Nonlinearity:

- Nonlinear Navier-Stokes equations in operator form:

$$\mathcal{L}(\boldsymbol{u}) = \boldsymbol{b} \qquad \text{with } \boldsymbol{u} = (\boldsymbol{v}, p)$$

- Disassemble as $\mathcal{L} = \mathcal{L}_A \oplus \mathcal{L}_V \oplus \mathcal{L}_G \oplus \mathcal{L}_D$, with operators $\mathcal{L}_A = \boldsymbol{v} \cdot \nabla \boldsymbol{v}$, $\mathcal{L}_V = -\nu \nabla^2 \boldsymbol{v}$, $\mathcal{L}_G = \nabla p$ and $\mathcal{L}_D = \nabla \cdot \boldsymbol{v}$
- Linearize $\mathcal{L}_A$ via a generalized Taylor expansion about current iterate of $\boldsymbol{v}^n$:

$$\mathcal{L}_A(\boldsymbol{v}) \approx \boldsymbol{v}^n \cdot \nabla \boldsymbol{v} + \boldsymbol{v} \cdot \nabla \boldsymbol{v}^n - \boldsymbol{v}^n \cdot \nabla \boldsymbol{v}^n$$

Data: $\mathcal{L}(\boldsymbol{u}) = \boldsymbol{b}$; initial guess for the unknowns: $\boldsymbol{u}^0 = (\boldsymbol{v}^0, p^0)$
while *not converged* **do**
  linearize nonliner system based on the current solution $\boldsymbol{u}^n$;
  $\boldsymbol{u}^{n+1} \leftarrow$ solve resulting system;
end

Algorithm 1: Nonlinear iteration loop

Governing equations

Unsteady incompressible Navier-Stokes equations in strong form:

$$
\begin{aligned}
\frac{\partial \boldsymbol{v}}{\partial t} - \nu\nabla^2\boldsymbol{v} + (\boldsymbol{v}\cdot\nabla)\boldsymbol{v} + \nabla p &= \boldsymbol{b} && \text{in } \Omega\times(0,T)\\
\nabla\cdot\boldsymbol{v} &= 0 && \text{in } \Omega\times(0,T)\\
\boldsymbol{v} &= \boldsymbol{v}_D && \text{on } \Gamma_D\times(0,T)\\
-p\boldsymbol{n} + \nu(\boldsymbol{n}\cdot\nabla)\boldsymbol{v} &= \boldsymbol{t} && \text{on } \Gamma_N\times(0,T)\\
\boldsymbol{v}(\boldsymbol{x},0) &= \boldsymbol{v}_0(\boldsymbol{x}) && \text{in } \Omega
\end{aligned}
$$

Variational problem: Find $\boldsymbol{v}(\boldsymbol{x},t) \in \boldsymbol{\mathcal{H}}^1_{\Gamma_D}(\Omega)\times(0,T)$ and $p(\boldsymbol{x},t)\in\mathcal{L}_2(\Omega)\times(0,T)$, such that for all $(\boldsymbol{w},q)\in\boldsymbol{\mathcal{H}}^1_{\Gamma_0}(\Omega)\times\mathcal{L}_2(\Omega)/\mathbb{R}$:

$$
\begin{cases}
(\boldsymbol{w},\boldsymbol{v}_t) + a(\boldsymbol{w},\boldsymbol{v}) + c(\boldsymbol{v};\boldsymbol{w},\boldsymbol{v}) + b(\boldsymbol{w},p) = (\boldsymbol{w},\boldsymbol{b}) + (\boldsymbol{w},\boldsymbol{t})_{\Gamma_N}\\
b(\boldsymbol{v},q) = 0
\end{cases}
$$

$$
\begin{cases}
\text{Find } \boldsymbol{v}^h \in \boldsymbol{\mathcal{H}}^1_{\Gamma_D}(\Omega)\cap\mathbf{V}_h^{TH}\times(0,T) \text{ and } p^h\in\mathcal{L}_2(\Omega)/\mathbb{R}\cap Q_h^{TH}\times(0,T),\\
\text{such that } \forall(\boldsymbol{w}^h,q^h)\in\boldsymbol{\mathcal{H}}^1_0(\Omega)\cap\mathbf{V}_h^{TH}\times\mathcal{L}_2(\Omega)/\mathbb{R}\cap Q_h^{TH}\\
(\boldsymbol{w}^h,\boldsymbol{v}^h_t) + a(\boldsymbol{w}^h,\boldsymbol{v}^h) + c(\boldsymbol{v}^h;\boldsymbol{w}^h,\boldsymbol{v}^h) + b(\boldsymbol{w}^h,p^h) = (\boldsymbol{w}^h,\boldsymbol{b}^h) + (\boldsymbol{w}^h,\boldsymbol{t}^h)_{\Gamma_N}\\
b(\boldsymbol{v}^h,q^h) = 0
\end{cases}
$$

Overview

Numerical experiments

1. Stokes flow problem with exact solution
2. Lid-driven cavity flow
3. Regularized lid-driven cavity flow
4. Steady flow around cylinder (Re 20)
5. Transient flow around cylinder (Re 100)

Stokes flow problem with exact solution

Find velocity field $\boldsymbol{v} = (v_1, v_2)$ and a pressure p on the square domain $\Omega = (0,1) \times (0,1)$ such that

$$\begin{aligned} -\nu \nabla^2 \boldsymbol{v} + \nabla p &= \boldsymbol{b} && \text{in } \Omega \\ \nabla \cdot \boldsymbol{v} &= 0 && \text{in } \Omega \\ \boldsymbol{v} &= \boldsymbol{v}_D && \text{on } \Gamma_D \end{aligned}$$

- kinematic viscosity $\nu = 1$
- Body force $\boldsymbol{b} = (b_1, b_2)$ and exact solution $\boldsymbol{v}^* = (v_1^*, v_2^*, p^*)$ taken from [9] as:

$$\begin{aligned} b_1 &= 6x + y\cos(xy) + 2\cos(y)\sin(x) \\ b_2 &= x\cos(xy) - 2\cos(x)\sin(y) \\ v_1^* &= \sin(x)\cos(y) \\ v_2^* &= -\sin(y)\cos(x) \\ p^* &= 3x^2 + \sin(xy) - 1.239811742000564725943866 \end{aligned}$$

Stokes flow problem with exact solution

L^2-errors of the velocity and pressure approximations obtained with isogeometric discretizations of various degrees and regularities:

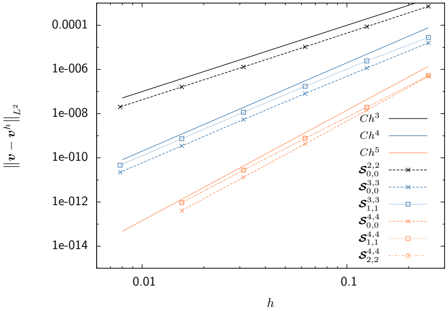

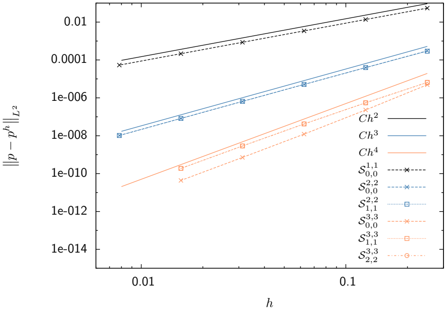

Remark

Optimal L^2-error convergence rates for velocity and pressure.

Lid-driven cavity flow

- Fluid in square cavity with height $H = 1$
- Steady incompressible Navier-Stokes equations
- no-slip Dirichlet b.c.'s ($\boldsymbol{u} = 0$) on the left, right and bottom walls
- Constant speed $U = 1$ at top wall
- Upper corners: Leaky vs. Non-leaky case
- Volumetric force $\boldsymbol{f} = \mathbf{0}$
- Fix discrete pressure field at one point or impose its average: $\int_\Omega p \, \mathrm{d}\Omega = 0$

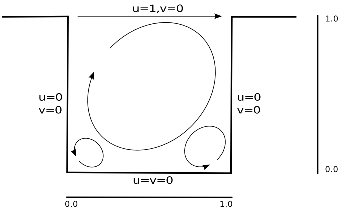

Figure : Sketch of lid-driven cavity model.

- Various B-spline space based discretizations for mesh refinement levels $h \in [1/32, 1/64, 1/128]$
- Comparisons with Ghia, highly accurate spectral results of Botella and two Isogeometric codes

Lid-driven cavity flow

Stream function (ψ) and vorticity (ω) profiles for Reynolds $100, 400$ and 1000 obtained with a $\boldsymbol{\mathcal{S}}^{2,2}_{0,0} \times \mathcal{S}^{1,1}_{0,0}$ discretization:

$$-\nabla^2\psi = \omega, \qquad \omega = \nabla \times \boldsymbol{v} = \frac{\partial v}{\partial x} - \frac{\partial u}{\partial y}$$

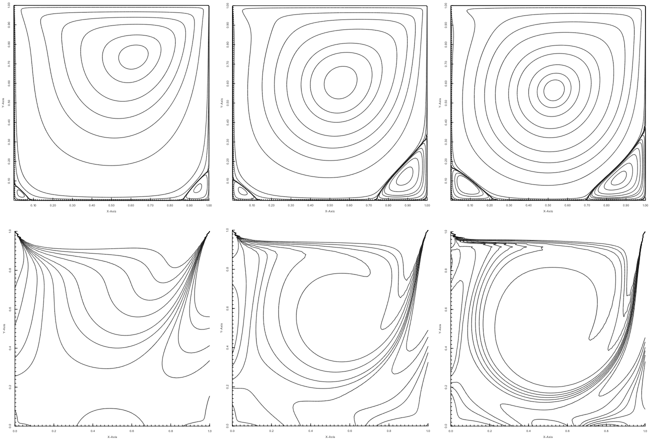

Lid-driven cavity flow

Re	Scheme	x	y	ψ	ω	N_{el}	h	N_{dof}	$N_{dof(vel.+pres.)}$	Grid points
100	$\mathcal{S}^{2,2}_{0,0} \times \mathcal{S}^{1,1}_{0,0}$	0.6150	0.7350	-0.103524	3.15526	32^2	1/32	9539	(8450+1089)	65^2
	$\mathcal{S}^{2,2}_{0,0} \times \mathcal{S}^{1,1}_{0,0}$	0.6150	0.7350	-0.103517	3.15350	64^2	1/64	37 507	(33282+4225)	129^2
	$\mathcal{S}^{2,2}_{0,0} \times \mathcal{S}^{1,1}_{0,0}$	0.6150	0.7350	-0.103516	3.15377	128^2	1/128	148 739	(132098+16641)	257^2
	$\mathcal{S}^{6,6}_{4,4} \times \mathcal{S}^{5,5}_{4,4}$	0.6150	0.7350	-0.103516	3.15382	32^2	1/32	10 891	(9522+1369)	69^2
	$\mathcal{S}^{6,6}_{4,4} \times \mathcal{S}^{5,5}_{4,4}$	0.6150	0.7350	-0.103516	3.15383	64^2	1/64	40 139	(35378+4761)	133^2
	$\mathcal{S}^{6,6}_{4,4} \times \mathcal{S}^{5,5}_{4,4}$	0.6150	0.7350	-0.103516	3.15383	128^2	1/128	153 931	(136242+17689)	261^2
	Ghia [11]	0.6172	0.7344	-0.103423	3.16646		1/128			129^2
	[8]	0.6150	0.7350	-0.103518			1/256			
400	$\mathcal{S}^{2,2}_{0,0} \times \mathcal{S}^{1,1}_{0,0}$	0.5550	0.6050	-0.114019	2.29555	32^2	1/32	9539	(8450+1089)	65^2
	$\mathcal{S}^{2,2}_{0,0} \times \mathcal{S}^{1,1}_{0,0}$	0.5550	0.6050	-0.113996	2.29470	64^2	1/64	37 507	(33282+4225)	129^2
	$\mathcal{S}^{2,2}_{0,0} \times \mathcal{S}^{1,1}_{0,0}$	0.5550	0.6050	-0.113989	2.29449	128^2	1/128	148 739	(132098+16641)	257^2
	$\mathcal{S}^{6,6}_{4,4} \times \mathcal{S}^{5,5}_{4,4}$	0.5550	0.6050	-0.113985	2.29448	32^2	1/32	10 891	(9522+1369)	69^2
	$\mathcal{S}^{6,6}_{4,4} \times \mathcal{S}^{5,5}_{4,4}$	0.5550	0.6050	-0.113988	2.29448	64^2	1/64	40 139	(35378+4761)	133^2
	$\mathcal{S}^{6,6}_{4,4} \times \mathcal{S}^{5,5}_{4,4}$	0.5550	0.6050	-0.113988	2.29448	128^2	1/128	153 931	(136242+17689)	261^2
	Ghia [11]	0.5547	0.6055	-0.113909	2.29469		1/256			257^2
	[8]	0.5550	0.6050	-0.114031			1/256			
1000	$\mathcal{S}^{2,2}_{0,0} \times \mathcal{S}^{1,1}_{0,0}$	0.5300	0.5650	-0.1189603	2.070030	32^2	1/32	9539	(8450+1089)	65^2
	$\mathcal{S}^{2,2}_{0,0} \times \mathcal{S}^{1,1}_{0,0}$	0.5300	0.5650	-0.1189511	2.067930	64^2	1/64	37 507	(33282+4225)	129^2
	$\mathcal{S}^{2,2}_{0,0} \times \mathcal{S}^{1,1}_{0,0}$	0.5300	0.5650	-0.1189400	2.067790	128^2	1/128	148 739	(132098+16641)	257^2
	$\mathcal{S}^{6,6}_{4,4} \times \mathcal{S}^{5,5}_{4,4}$	0.5300	0.5650	-0.1189165	2.067510	32^2	1/32	10 891	(9522+1369)	69^2
	$\mathcal{S}^{6,6}_{4,4} \times \mathcal{S}^{5,5}_{4,4}$	0.5300	0.5650	-0.1189341	2.067710	64^2	1/64	40 139	(35378+4761)	133^2
	$\mathcal{S}^{6,6}_{4,4} \times \mathcal{S}^{5,5}_{4,4}$	0.5300	0.5650	-0.1189360	2.067730	128^2	1/128	153 931	(136242+17689)	261^2
	Botella [10]	0.5308	0.5652	-0.1189249	2.067396		1/48			N $= 48$
	Botella [10]	0.5308	0.5652	-0.1189366	2.067750		1/96			N $= 96$
	Botella [10]	0.5308	0.5652	-0.1189366	2.067753		1/160			N $= 160$
	Ghia [11]	0.5313	0.5625	-0.1179290	2.049680		1/128			129^2
	[8]	0.5300	0.5650	-0.1185110			1/256			

Table : Location, stream function and vorticity of the primary vortex.

Lid-driven cavity flow

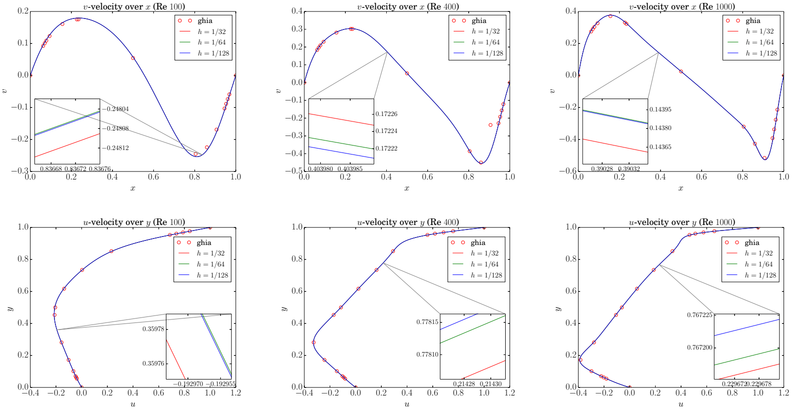

Figure : Profiles of v- and u-velocity components over horizontal and vertical lines through geometric center of the cavity for Re $100, 400$ and 1000. Discretization: $\boldsymbol{\mathcal{S}}_{0,0}^{2,2} \times \mathcal{S}_{0,0}^{1,1}$

Lid-driven cavity flow

Re	Center line	Property	$\boldsymbol{\mathcal{S}}^{2,2}_{0,0} \times \mathcal{S}^{1,1}_{0,0}(h = 1/128)$	Botella [10]	Ghia [11]	[12] $(h = 1/128)$	[8] $(h = 1/256, p = 2)$
100	Vertical	u_{min}	−0.214 04	−0.214 04	−0.210 90	−0.214 14	−0.214 02
	$(x = 0.5)$	y-coord	0.4578	0.4581	0.4531		0.4600
	Horizontal	v_{min}	−0.253 80	−0.253 80	−0.245 33	−0.253 87	−0.253 71
	$(y = 0.5)$	x-coord	0.8112	0.8104	0.8047		0.8100
		v_{max}	0.179 57	0.179 57	0.175 27	0.179 66	0.179 53
		x-coord	0.2369	0.2370	0.2344		0.2350
400	Vertical	u_{min}	−0.328 72		−0.327 26	−0.329 89	−0.328 80
	$(x = 0.5)$	y-coord	0.2811		0.2813		0.2800
	Horizontal	v_{min}	−0.454 02		−0.449 93	−0.454 70	−0.453 86
	$(y = 0.5)$	x-coord	0.8635		0.8594		0.8600
		v_{max}	0.303 83		0.302 03	0.304 71	0.303 93
		x-coord	0.2249		0.2266		0.2250
1000	Vertical	u_{min}	−0.388 57	−0.388 53	−0.382 89	−0.390 21	−0.387 54
	$(x = 0.5)$	y-coord	0.1727	0.1717	0.1719		0.1700
	Horizontal	v_{min}	−0.526 92	−0.527 07	−0.515 50	−0.528 84	−0.525 82
	$(y = 0.5)$	x-coord	0.9076	0.9092	0.9063		0.9100
		v_{max}	0.376 94	0.376 94	0.370 95	0.378 56	0.375 72
		x-coord	0.1566	0.1578	0.1563		0.1600

Table : Extrema of the velocity components w.r.t vertical and horizontal lines through the geometric center of the cavity for Re $100, 400$ and 1000.

Lid-driven cavity flow

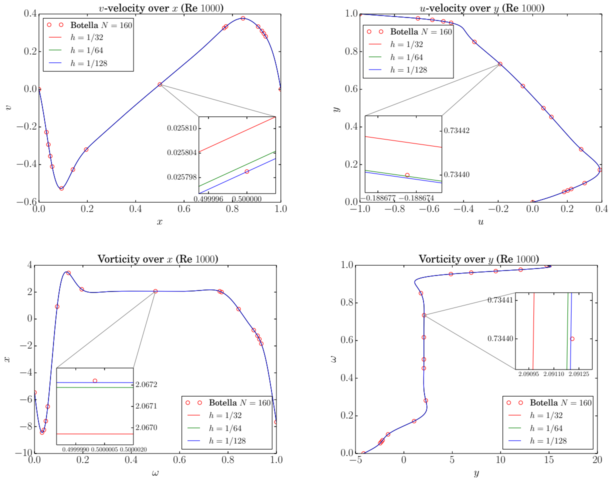

Figure : Profiles of v- and u-velocity components and vorticity over horizontal and vertical lines through geometric center of the cavity for Re 1000. Discretization: $\boldsymbol{\mathcal{S}}^{6,6}_{4,4} \times \mathcal{S}^{5,5}_{4,4}$

Regularized lid-driven cavity flow

Parabolic velocity profile on top boundary to avoid jumps in velocity function:

$$\mathbf{u}_{lid} = [-16x^2(1-x)^2, 0]$$

Extend analysis to global quantities, such as KINETIC ENERGY (E) and ENSTROPHY (Z).

$$E = \frac{1}{2}\int_{\Omega} \|\mathbf{u}\|^2 \,\mathrm{d}x$$

$$Z = \frac{1}{2}\int_{\Omega} \omega^2 \,\mathrm{d}x$$

Regularized lid-driven cavity flow

Scheme	Kinetic Energy	Enstrophy	N$_{el}$	h	N$_{dof}$	N$_{dof(vel.\ +\ pres.)}$	Grid points
$\boldsymbol{\mathcal{S}}_{0,0}^{2,2} \times \mathcal{S}_{0,0}^{1,1}$	0.022909	4.80747	32^2	$1/32$	9539	(8450+1089)	65^2
	0.022778	4.82950	64^2	$1/64$	37507	(33282+4225)	129^2
	0.022767	4.83041	128^2	$1/128$	148739	(132098+16641)	257^2
	0.022767	4.83043	256^2	$1/256$	592387	(526338+66049)	513^2
$\boldsymbol{\mathcal{S}}_{0,0}^{3,3} \times \mathcal{S}_{0,0}^{2,2}$	0.022905	4.81717	16^2	$1/16$	5891	(4802+1089)	49^2
	0.022773	4.83079	32^2	$1/32$	23043	(18818+4225)	97^2
	0.022767	4.83047	64^2	$1/64$	91139	(74498+16641)	193^2
	0.022767	4.83042	128^2	$1/128$	362499	(296450+66049)	385^2
$\boldsymbol{\mathcal{S}}_{1,1}^{3,3} \times \mathcal{S}_{1,1}^{2,2}$	0.022777	4.82954	32^2	$1/32$	9868	(8712+1156)	66^2
	0.022767	4.83048	64^2	$1/64$	38156	(33800+4356)	130^2
	0.022767	4.83046	128^2	$1/128$	150028	(133128+16900)	258^2
Ref. [13] (Bruneau)	0.021564	4.6458					64^2
	0.022315	4.7711					128^2
	0.022542	4.8123					256^2
	0.022607	4.8243					512^2
Ref. [14] ([4]Q_2P_1 FE)	0.022778	4.82954	64^2	$1/64$			
	0.022768	4.83040	128^2	$1/128$			
	0.022766	4.83050	256^2	$1/256$			

Table : Kinetic energy and enstrophy of the regularized cavity flow for Reynolds 1000.

[4] Velocity: Biquadratic, continuous; Pressure: Linear (value and two partial derivatives), discontinuous

Regularized lid-driven cavity flow

Re	h	$\boldsymbol{\mathcal{S}}_{0,0}^{2,2} \times \mathcal{S}_{0,0}^{1,1}$	[5] $\tilde{Q}_1 Q_0$ FE	$Q_2 P_1$ FE	[6] W-LSFE Q_2 [14]
1	1/64	1.862439E-02	1.860621E-02	1.862439E-02	1.862353E-02
	1/128	1.862438E-02	1.861982E-02	1.862438E-02	1.862432E-02
	1/256	1.862438E-02	1.862324E-02	1.862438E-02	1.862438E-02
400	1/64	2.131703E-02	2.148649E-02	2.131707E-02	2.133053E-02
	1/128	2.131547E-02	2.136484E-02	2.131547E-02	2.131581E-02
	1/256	2.131537E-02	2.132812E-02	2.131529E-02	2.131537E-02
1000	1/64	2.277788E-02	2.409799E-02	2.277778E-02	2.552796E-02
	1/128	2.276761E-02	2.305179E-02	2.276761E-02	2.287704E-02
	1/256	2.276692E-02	2.282649E-02	2.276582E-02	2.277389E-02

Table : Convergence of approximated kinetic energy for the regularized cavity flow problem.

[5] Velocity: Bilinear, rotated; Pressure: Constant

[6] Biquadratic Least-Square finite elements

Flow around cylinder

- Testcase 1: Steady flow around cylinder (Re 20)
- Testcase 2: Transient flow around cylinder (Re 100)
- Same geometry for both test cases
- Geometry: pipe without a circular cylinder of radius $r = 0.05$
- $\Omega = (0, 2.2) \times (0, 0.41) \setminus B_r(0.2, 0.2)$
- Cylinder centered around $(x, y) = (0.2, 0.2)$
- Parabolic inflow profile $u(0, y) = \left(\frac{4Uy(0.41-y)}{0.41^2}, 0 \right)$
- Flow characteristic length: $D = 2r = 0.1$
- Fluid density $\rho = 1$, Fluid kinematic viscosity $\nu = 0.001$
- No-slip b.c.'s on the lower and upper walls $\Gamma_1 = (0, 2.2) \times \{0\}$ and $\Gamma_3 = (0, 2.2) \times \{0.41\}$ and on boundary $S = \partial B_r(0.2, 0.2)$: $u_{|\Gamma_1} = u_{|\Gamma_3} = u_{|S} = 0$
- "do-nothing" boundary conditions, $-p\boldsymbol{n} + \nu(\boldsymbol{n} \cdot \nabla)\boldsymbol{v} = \boldsymbol{0}$, on outflow boundary $\Gamma_2 = \{2.2\} \times (0, 0.41)$

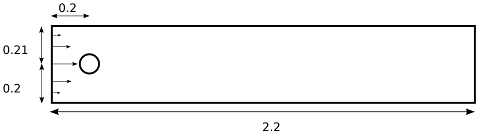

Flow around cylinder

Computation of Drag and Lift coefficients: C_D, C_L

- S: surface of the obstacle
- $\boldsymbol{n}_S$: outer normal vector of the obstacle
- tangent vector $\boldsymbol{\tau} := (n_y, -n_x)^T$
- $\boldsymbol{u}_\tau := \boldsymbol{u} \cdot \boldsymbol{\tau}$

$$\boldsymbol{F}_T = \int_S \sigma \boldsymbol{n}_S \, ds$$

$$\sigma := -p\boldsymbol{I} + \mu[\nabla \boldsymbol{u} + (\nabla \boldsymbol{u})^T] \qquad \text{(Total stress tensor)}$$

$$F_D = \int_S \left(\rho\nu \frac{\partial \boldsymbol{u}_\tau}{\partial \boldsymbol{n}_S} n_y - p n_x \right) ds, \qquad F_L = -\int_S \left(\rho\nu \frac{\partial \boldsymbol{u}_\tau}{\partial \boldsymbol{n}_S} n_x + p n_y \right) ds$$

$$C_D = \frac{2}{\rho \bar{U}^2 D} F_D, \qquad C_L = \frac{2}{\rho \bar{U}^2 D} F_L$$

Flow around cylinder

Volume integral approach:

$$\boldsymbol{v}_{d|S} = (1,0)^T, \boldsymbol{v}_{d|\bar{\Omega}-S} = \mathbf{0}, \qquad \boldsymbol{v}_{l|S} = (0,1)^T, \boldsymbol{v}_{l|\bar{\Omega}-S} = \mathbf{0}$$

$$C_D = -\frac{2}{\rho \bar{U}^2 D}\left[(\nu \nabla \boldsymbol{u}, \nabla \boldsymbol{v_d}) - (p, \nabla \cdot \boldsymbol{v_d})\right]$$

$$C_L = -\frac{2}{\rho \bar{U}^2 D}\left[(\nu \nabla \boldsymbol{u}, \nabla \boldsymbol{v_l}) - (p, \nabla \cdot \boldsymbol{v_l})\right]$$

Discrete setting:

$$C_D = -\frac{2}{\rho \bar{U}^2 D}\left[\mathbf{D}_u \cdot \mathbf{u}_u + \mathbf{G_u} \cdot \mathbf{p}\right] \cdot \mathbf{v}_d$$

$$C_L = -\frac{2}{\rho \bar{U}^2 D}\left[\mathbf{D}_v \cdot \mathbf{u}_v + \mathbf{G_v} \cdot \mathbf{p}\right] \cdot \mathbf{v}_l$$

$$\begin{pmatrix} \mathbf{D}_u & & \mathbf{G_u} \\ & \mathbf{D}_v & \mathbf{G_v} \\ \mathbf{G}_u^T & \mathbf{G}_v^T & \end{pmatrix}, \begin{pmatrix} \mathbf{u}_u \\ \mathbf{u}_v \\ \mathbf{p} \end{pmatrix}, \begin{pmatrix} \mathbf{v}_d \\ \mathbf{v}_l \\ \end{pmatrix}$$

Flow around cylinder

Computational domain modeled as multipatch NURBS mesh:

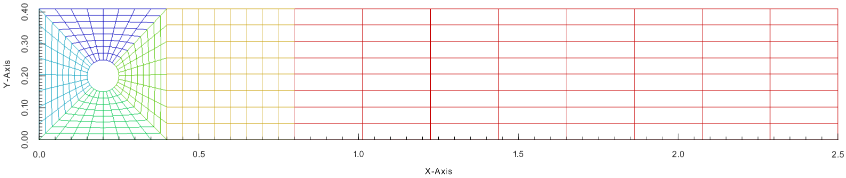

Figure : Multi-patch NURBS mesh for flow around cylinder at refinement level 3. Each uniquely colored initial 1×1 element patch has been refined three times, giving rise to 8×8 elements in each patch, eventually.

Parabolic inflow condition imposed via finite element L^2-projection of profile f on control variables of left boundary Γ_4:

$$\int_{\Gamma_4} (f - P_h f)\, w \,\mathrm{d}\Gamma_4 = 0, \quad \forall w \in \mathcal{W}_h$$

Steady flow around cylinder (Re 20)

- $U = 0.3$
- $\bar{U} = \frac{2}{3}U = 0.2$
- $\mathrm{Re} = \frac{\bar{U}D}{\nu} = \frac{0.2 \cdot 0.1}{0.001} = 20$
- Isogeometric discretizations: $\boldsymbol{\mathcal{S}}^{3,3}_{0,0} \times \mathcal{S}^{2,2}_{0,0}$, $\boldsymbol{\mathcal{S}}^{3,3}_{1,1} \times \mathcal{S}^{2,2}_{1,1}$

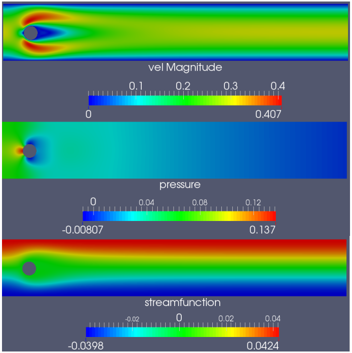

Steady flow around cylinder (Re 20)

Scheme	C_D	C_L	Δp	N_{dof}	N_{el}	Level
$\boldsymbol{\mathcal{S}}^{3,3}_{0,0} \times \mathcal{S}^{2,2}_{0,0}$	5.645768	0.0067650	0.11675114	8832	384	L3
$\boldsymbol{\mathcal{S}}^{3,3}_{0,0} \times \mathcal{S}^{2,2}_{0,0}$	5.594618	0.0095045	0.11733243	34560	1536	L4
$\boldsymbol{\mathcal{S}}^{3,3}_{0,0} \times \mathcal{S}^{2,2}_{0,0}$	5.582119	0.0104074	0.11749107	136704	6144	L5
$\boldsymbol{\mathcal{S}}^{3,3}_{0,0} \times \mathcal{S}^{2,2}_{0,0}$	5.579918	0.0105860	0.11751658	543744	24576	L6
$\boldsymbol{\mathcal{S}}^{3,3}_{0,0} \times \mathcal{S}^{2,2}_{0,0}$	5.579588	0.0106143	0.11751977	2168832	98304	L7
$\boldsymbol{\mathcal{S}}^{3,3}_{0,0} \times \mathcal{S}^{2,2}_{0,0}$	5.579543	0.0106183	0.11752012	8663040	393216	L8
$\boldsymbol{\mathcal{S}}^{3,3}_{1,1} \times \mathcal{S}^{2,2}_{1,1}$	5.647333	0.0066836	0.11633509	4212	384	L3
$\boldsymbol{\mathcal{S}}^{3,3}_{1,1} \times \mathcal{S}^{2,2}_{1,1}$	5.594742	0.0095065	0.11723232	15300	1536	L4
$\boldsymbol{\mathcal{S}}^{3,3}_{1,1} \times \mathcal{S}^{2,2}_{1,1}$	5.582148	0.0104082	0.11749043	58212	6144	L5
$\boldsymbol{\mathcal{S}}^{3,3}_{1,1} \times \mathcal{S}^{2,2}_{1,1}$	5.579918	0.0105861	0.11751770	226980	24576	L6
$\boldsymbol{\mathcal{S}}^{3,3}_{1,1} \times \mathcal{S}^{2,2}_{1,1}$	5.579588	0.0106143	0.11751993	896292	98304	L7
$\boldsymbol{\mathcal{S}}^{3,3}_{1,1} \times \mathcal{S}^{2,2}_{1,1}$	5.579543	0.0106183	0.11752014	3562020	393216	L8
Ref.	5.57953523384	0.010618948146	0.11752016697			

$\mathcal{C}^1$ vs. $\mathcal{C}^0$ DOF percentage ratio (DOFs$(\boldsymbol{\mathcal{S}}^{3,3}_{1,1} \times \mathcal{S}^{2,2}_{1,1}, L)/$DOFs$(\boldsymbol{\mathcal{S}}^{3,3}_{0,0} \times \mathcal{S}^{2,2}_{0,0}, L) * 100)$ for level L:

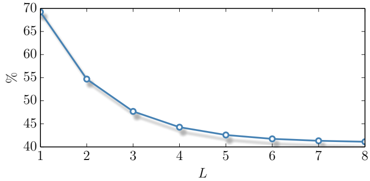

Steady flow around cylinder (Re 20)

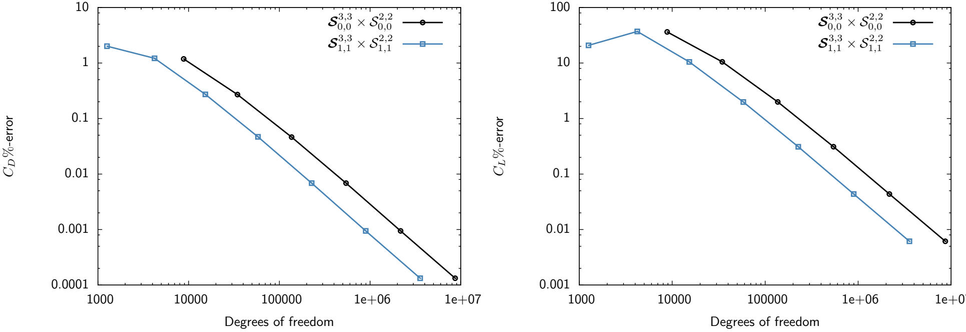

Remark

$\boldsymbol{\mathcal{S}}_{1,1}^{3,3} \times \mathcal{S}_{1,1}^{2,2}$ superior to $\boldsymbol{\mathcal{S}}_{0,0}^{3,3} \times \mathcal{S}_{0,0}^{2,2}$ accuracy wise.

Transient flow around cylinder (Re 100)

- Simulate time periodic behavior
- Drag, lift, pressure drop, lift profile frequency f, Strouhal number St $= \frac{Df}{\bar{U}}$
- $U = 1.5$
- $\bar{U} = \frac{2}{3}U = 1$
- Re $= \frac{\bar{U}D}{\nu} = \frac{\frac{2}{3}\cdot\frac{3}{2}\cdot\frac{1}{10}}{\frac{1}{1000}} = 100$
- Isogeometric space discretization: $\boldsymbol{\mathcal{S}}^{3,3}_{0,0} \times \mathcal{S}^{2,2}_{0,0}$
- Time discretization: θ-scheme with $\theta = 0.5 \Rightarrow 2$-nd order accurate implicit Crank-Nicolson scheme

Solved in a fully coupled manner:

$$\begin{pmatrix} \frac{1}{\Delta t}\mathbf{M} + \theta(\mathbf{D} + \mathbf{C}(v^{n+1})) & \mathbf{G} \\ \mathbf{G}^T & \mathbf{0} \end{pmatrix} \begin{pmatrix} \mathbf{v}^{n+1} \\ \mathbf{p}^{n+1} \end{pmatrix} = \begin{pmatrix} \frac{1}{\Delta t}\mathbf{M} - (1-\theta)(\mathbf{D} + \mathbf{C}(v^{n})) & \mathbf{0} \\ \mathbf{0} & \mathbf{0} \end{pmatrix} \begin{pmatrix} \mathbf{v}^{n} \\ \mathbf{p}^{n} \end{pmatrix}$$
$$+ \theta \mathbf{f}^{n+1} + (1-\theta)\mathbf{f}^{n}.$$

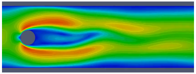

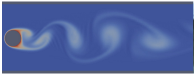

Transient flow around cylinder (Re 100)

Convergence of min-C_D, max-C_D, mean-C_D, amp-C_D, min-C_L, max-C_L, mean-C_L and amp-C_L, f and St to a Q_2P_1 FE reference solution:

Level	Δt	min-C_D(Abs-Err,%-Err)	max-C_D(Abs-Err,%-Err)	mean-C_D(Abs-Err,%-Err)	amp-C_D(Abs-Err,%-Err)
L4	$1/400$	3.2216 (0.0573, 1.81)	3.2857 (0.0583, 1.81)	3.2536 (0.0578, 1.81)	0.0642 (0.0011, 1.62)
L5	$1/400$	3.1755 (0.0112, 0.35)	3.2392 (0.0118, 0.37)	3.2074 (0.0116, 0.36)	0.0637 (0.0006, 0.94)
L6	$1/400$	3.1665 (0.0022, 0.07)	3.2300 (0.0026, 0.08)	3.1983 (0.0025, 0.08)	0.0635 (0.0004, 0.58)
Ref. [15]		3.1643	3.2274	3.1958	0.0631

Level	Δt	min-C_L(Abs-Err,%-Err)	max-C_L(Abs-Err,%-Err)	mean-C_L(Abs-Err,%-Err)	amp-C_L(Abs-Err,%-Err)
L4	$1/400$	-1.0302 (0.0089, 0.87)	0.9903 (0.0037, 0.38)	-0.01995 (0.00259, 14.92)	2.0206 (0.0127, 0.63)
L5	$1/400$	-1.0249 (0.0036, 0.35)	0.9890 (0.0024, 0.25)	-0.01794 (0.00058, 3.34)	2.0139 (0.0060, 0.30)
L6	$1/400$	-1.0242 (0.0029, 0.28)	0.9893 (0.0027, 0.27)	-0.01747 (0.00011, 0.63)	2.0135 (0.0056, 0.28)
Ref. [15]		-1.0213	0.9866	-0.01736	2.0079

Level	Δt	$1/f$	St
L4	$1/400$	0.33250	0.30075
L5	$1/400$	0.33250	0.30075
L6	$1/400$	0.33000	0.30303
Ref. [15]		0.33125	0.30189

Transient flow around cylinder (Re 100)

Convergence of the drag profile to a Q_2P_1 FE reference solution:

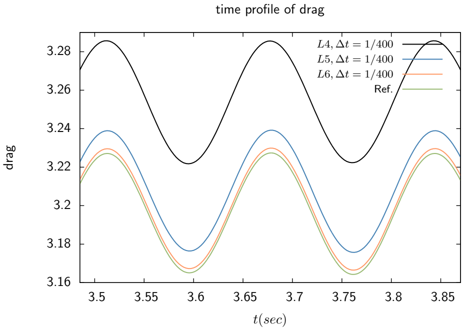

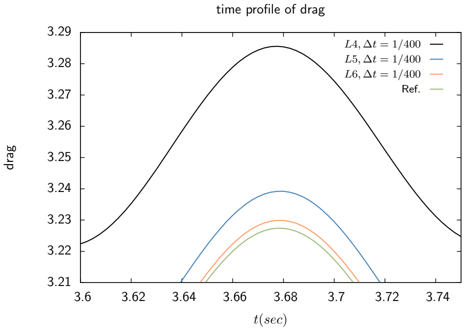

Transient flow around cylinder (Re 100)

Convergence of the lift profile to a Q_2P_1 FE reference solution:

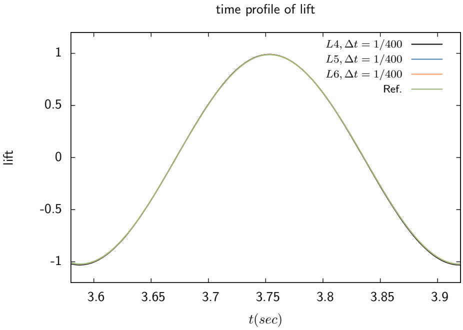

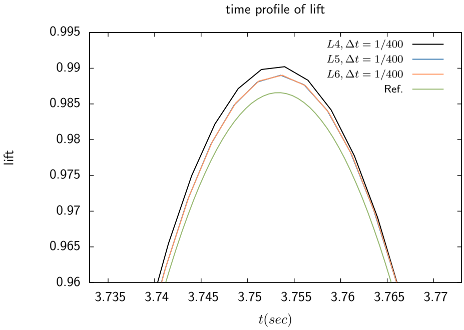

Transient flow around cylinder (Re 100)

Convergence of the pressure drop profile to a Q_2P_1 FE reference solution:

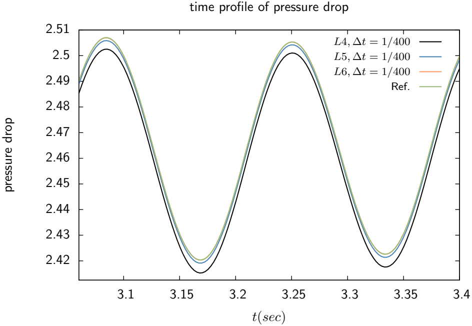

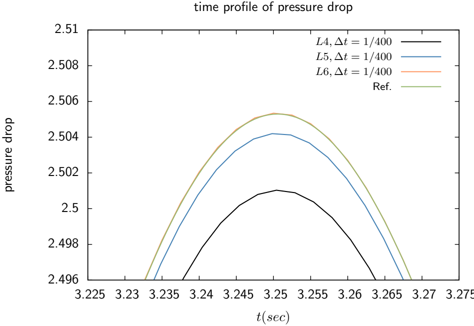

Outlook

- Multiphysics
  - Multiphase flow combined with Phase Field models (Cahn-Hilliard,etc.)
  - Fluid Solid Interaction (Arbitrary Lagrangian Eulerian, Fictitious Boundary Method)
  - Non-Newtonian fluids
  - ...
- Local refinement (Hierarchical B-splines, T-splines, etc.)
- Multigrid

References

T-Splines
http://www.tsplines.com

Thomas W. Sederberg et al.
Watertight Trimmed NURBS

Yongjie Zhang et al.
Patient-Specific Vascular NURBS Modeling for Isogeometric Analysis of Blood Flow.

J. Austin Cottrell and Thomas J.R. Hughes and Yuri Bazilevs
Isogeometric Analysis. Toward Integration of CAD and FEA

Y. Bazilevs, L. Beirão Da Veiga, J.A. Cottrell, T.J.R. Hughes and G. Sangalli
Isogeometric Analysis: Approximation, stability and error estimates for h-refined meshes

Anna Tagliabue
Isogeometric Analysis for reduced Fluid-Structure Interaction models in Haemodynamic applications

Babak Sayyid Hosseini, Matthias Möller and Stefan Turek
Isogeometric Analysis of the Navier-Stokes equations with Taylor-Hood B-spline elements

Anna Tagliabue, Luca Dedè, Alfio Quarteroni
Isogeometric Analysis and Error Estimates for High Order Partial Differential Equations in Fluid Dynamics

C. de Falco, A. Reali, and R. Vázquez
GeoPDEs: a research tool for Isogeometric Analysis of PDEs. Adv. Eng. Softw., 42(12):1020-1034, 2011.

O. Botella et al.
Benchmark spectral results on the lid-driven cavity flow

Ghia et al.
High-Re Solutions for Incompressible Flow using the Navier-Stokes Equations and a Multigrid Method

J.A. Evans and T.J.R. Hughes
Isogeometric Divergence-conforming B-splines for the Steady Navier-Stokes Equations

C.-H. Bruneau et al.
The 2D lid-driven cavity problem revisited

M. Nickaeen et al.
Newton multigrid least-squares FEM for the V-V-P formulation of the Navier-Stokes equations

FeatFlow CFD Benchmarking
http://www.featflow.de/en/benchmarks/cfdbenchmarking/flow/dfg_benchmark2_re100.html

Appendix

Data: $\mathcal{S}^{p,p}_{\alpha,\alpha}$, $\mathcal{Q}$, $\mathbf{F}$

while *not processed all patches* **do**

  while *not processed all elements* $e \in \mathcal{Q}_{patch}$ **do**

    while *not processed all element cubature points* $\boldsymbol{q}$ **do**

      - project $\boldsymbol{q} \in \tilde{\Omega}$ to parametric spline domain $\hat{\Omega}$: $\hat{\boldsymbol{q}} = T(\boldsymbol{q}, e)$

      - compute Deformation tensor $\mathbf{DF}$, its determinant $\det(\mathbf{DF})$ and its inverse transpose $(\mathbf{DF})^{-T}$

      - pull back integrals from Ω to the parametric spline domain:

      $$\int_a^b f(g(\xi))g'(\xi)\, d\xi = \int_{g(a)}^{g(b)} f(x)\, dx$$

      express all functions w.r.t parametric coordinates

      $$\nabla_x u(x) = (\mathbf{DF})(\xi)^{-T} \nabla_\xi u(\xi)$$

      - evaluate integrands for $\hat{\boldsymbol{q}}$

      - update system matrices and rhs vector

    end

  end

end

Algorithm 2: Assembly in IGA

Appendix

Transformation T from reference to parametric domain:

$$\xi = T(\tilde{\xi}, \xi_{\text{left}}, \xi_{\text{right}}) = ((1-\tilde{\xi})/2)\cdot\xi_{\text{left}} + ((1+\tilde{\xi})/2)\cdot\xi_{\text{right}} \qquad \tilde{\xi} \in [-1, 1]$$

Deformation tensor of geometrical mapping:

$$\mathbf{DF} = \begin{pmatrix} \frac{\partial x}{\partial \xi} & \frac{\partial x}{\partial \eta} \\ \frac{\partial y}{\partial \xi} & \frac{\partial y}{\partial \eta} \end{pmatrix} = \begin{pmatrix} \sum_{i=1}^{n}\sum_{j=1}^{m} N'_{i,p}(\xi)M_{j,q}(\eta)\boldsymbol{P}^x_{i,j} & \sum_{i=1}^{n}\sum_{j=1}^{m} N_{i,p}(\xi)M'_{j,q}(\eta)\boldsymbol{P}^x_{i,j} \\ \sum_{i=1}^{n}\sum_{j=1}^{m} N'_{i,p}(\xi)M_{j,q}(\eta)\boldsymbol{P}^y_{i,j} & \sum_{i=1}^{n}\sum_{j=1}^{m} N_{i,p}(\xi)M'_{j,q}(\eta)\boldsymbol{P}^y_{i,j} \end{pmatrix}$$

$$\mathbf{DF}^{-1} = \begin{pmatrix} \frac{\partial \xi}{\partial x} & \frac{\partial \xi}{\partial y} \\ \frac{\partial \eta}{\partial x} & \frac{\partial \eta}{\partial y} \end{pmatrix} = \frac{1}{\det(\mathbf{DF})} \begin{pmatrix} \frac{\partial y}{\partial \eta} & -\frac{\partial x}{\partial \eta} \\ -\frac{\partial y}{\partial \xi} & \frac{\partial x}{\partial \xi} \end{pmatrix}$$

Appendix

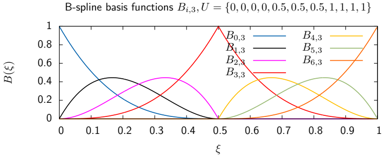

(i) $\mathcal{S}_0^3$

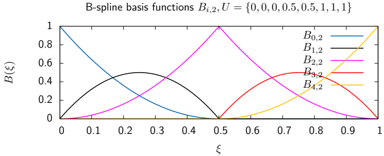

(j) $\mathcal{S}_0^2$

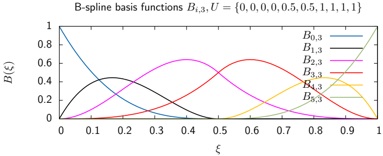

(k) $\mathcal{S}_1^3$

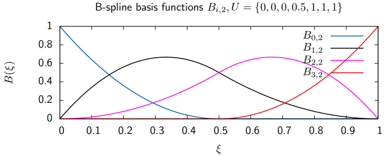

(l) $\mathcal{S}_1^2$

Appendix

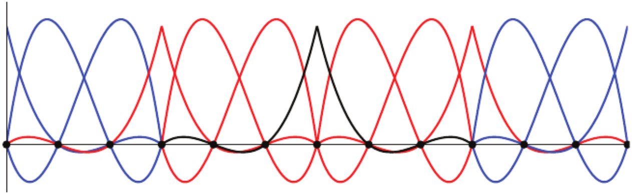

(a) Standard cubic finite element basis functions with equally spaced nodes

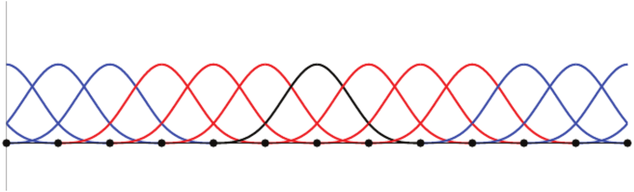

(b) Cubic B-spline basis functions with equally spaced knots

Figure : Courtesy of Hughes et al.